DESIGN OF A LOW FRINGE FIELD SEPTUM MAGNET FOR USE AT THE CERN - ISR*

L. G. Ratner, R. J. Lari, J. A. Bywater, E. C. Berrill
Argonne National Laboratory
Argonne, Illinois 60439

Abstract

A 1.2 m long x 5 cm high x 50 cm wide gap magnet with a field integral of 18 kG-meters was required to be placed within 5 cm of the Intersecting Storage Rings (ISR) circulating beam for the Argonne-Bologna-Michigan experiment at intersection region II. To preserve the circulating beam in the ISR, it is necessary to keep the fringe field gradient to less than 0.005 kG-meters/cm. This was accomplished by an independent, external correction coil which reduced the field in the coil retaining plate, thus reducing the leakage field.

During actual operation at the CERN - ISR, the correction coils performed as predicted. They were indeed necessary to prevent ISR beam losses and it would not have been possible to perform the experiment without them.

This paper describes the utilization of the computer program TRIM to determine the iron, copper and correction coil winding configuration to achieve these conditions. The mechanical/electrical design and actual magnetic measurements obtained from the completed magnet are presented.

Theory of the Correction Coils

In most septum magnets, the septum part of the coil is constrained by a coil retaining plate as seen in Figures 1 and 2. The retaining plate for this magnet is 1 cm thick by 25 cm high. As the current increases in the main coil, the flux density, B, in the retaining plate increases. The two flux paths labeled A and B in Figure 3 illustrate the direction of the field when the main coil (I_M) is energized. At 15 kG the H field in 1010 steel is 10 oersteds and at 18 kG the H field is 102 oersteds. Since the tangential components of H are continuous at the surface of the retaining plate, the leakage field for 15 and 18 kG are approximately 10 and 100 G.

When correction coils (I_C) are energized having current directions as shown in Figure 3, the flux paths labeled C and D are possible. However, since the reluctance of path C is much larger than path D most of the flux produced by the correction coils will follow path D. Note that in the coil retaining plate, the flux due to the correction coil and main coil is in opposite directions. Hence, it is possible to adjust the correction coil to cancel most of the field in the coil retaining plate which was produced by the main coil and thus reduce the leakage field to a negligible value. The placement of the turns in the correction coil approximates a toroidal winding. This method has been successfully used in the ZGS extraction system magnets.[1,2]

Computer Design of the Correction Coils

The computer program TRIM[3,4] was used to calculate the vector magnetic potential at each of the 1161 mesh points shown in Figure 4. For a central field of 15 kG and no correction coil current, the flux distribution is as shown in Figure 5. Notice that only one of the 50 flux lines plotted has the direction of path B, Figure 3. The field in the coil retaining plate is -17742 G producing a leakage field of -89 G in the air. This is shown in Figure 6. To reduce the leakage field to a negligible value, a correction coil current of 401 amp turns per pole was required. The ratio of ampere turns NI_C/NI_M was 0.013.

For a central field of 17,500 G, the coil retaining plate field was 18,635 G and produced a leakage field of -143 G at the plate. A correction coil current of 880 amp turns overcorrected the field in the retaining plate and produced a positive leakage field of 11 G at the plate. For this case, the ratio of NI_C/NI_M was 0.025.

Very small errors in the calculation of the vector potentials will produce large errors in the calculation of the leakage field with this coarse mesh. The error in small leakage field calculations could be as much as a factor of 5 times the value calculated. Hence, it was desirable to keep the ratio of NI_C/NI_M as small as possible, with the anticipation of increasing NI_C, by as much as a factor of 5. Choosing a finer mesh and smaller residual would reduce this factor.

*Work performed under the auspices of the U. S. Atomic Energy Commission.

The effective length of this magnet has also been calculated by TRIM using a method described elsewhere[5] in these proceedings. The value of 123.55 cm agrees very well with the measurements of 123.57 cm.

Mechanical and Electrical Design

The final design of the magnet was based on the computer design requirements. The main and correction coil conductors were matched to an existing CERN 250 V - 900 A power supply utilizing existing conductor on hand at ANL. Table I summarizes the basic magnet design data and Table II shows the calculated operating conditions for the magnet.

The main coil was constructed as two symmetrical halves of 40 turns each. Individual turns were fabricated from two sizes of conductor as shown in Figure 7. The smaller conductor was utilized for the septum leg to minimize the over-all width while the larger size conductor, used for the return leg, reduced the total voltage required for the magnet to acceptable limits. Each coil half contains five conductor layers with eight turns in each layer. The turns were formed to the required size and insulated with 0.13 mm fiber glass tape applied half lapped. The turns were connected in series by silver brazing adjacent turns in the 90^{o} crossover area on the terminal end. After brazing, ground insulation of 0.13 mm fiber glass tape was applied half lapped, the insulated coil was placed in a steel form and vacuum impregnated with the following epoxy resin formulation.

Ingredient	Manufacturer	Parts by Weight
Epon 826 Resin	Shell Chem. Co.	50
DER 736 Resin	Dow Chem. Co.	50
Tonox Curing Agent	U.S. Rubber Co.	28

The steel core was fabricated from AISI 1010 hot rolled steel plate. All plate used in the core fabrication was heat treated and ultrasonically inspected to insure adequate magnetic properties. The core was split on the mid plane for machining and assembly reasons.

At final assembly the corresponding main coil and core halves were assembled and the correction coil wound onto the core. The two halves were then assembled and the coils connected electrically with solid bus bar. Separate power terminals were provided for the main and correction coil. Water circuits were connected in parallel to the manifolds with rubber hose.

Magnetic Field Measurements

The high speed data acquisition system used to measure this magnet has been described elsewhere.[6,7,8] In Figure 8, the $\int Bd\ell$ is shown as a function of main coil current and is seen to be linear over the region of interest. Figure 9 shows the leakage $\int Bd\ell$ as calculated by TRIM and as measured with no correction coil current. Figure 10 shows the results with the correction coil. The optimum correction coil current to use for a given main coil current is shown in Figure 11. As seen in this figure, the ratio NI_C/NI_M is about three times larger than calculated for a current of about 750 amps. The excellent agreement between the calculated and measured effective length is shown in Figure 12.

Summary and Conclusions

The theory of correction coils to reduce the leakage field of a septum magnet has been explained. A computer design and mechanical and electrical design were presented as well as the actual magnetic measurements on the finished magnet. The magnet performed well for the Argonne-Bologna-Michigan experiment at the CERN-ISR during 1971.

Acknowledgments

The authors are indebted to T. Hardek and J. Lewellen for their assistance in obtaining the magnetic field measurements; to D. Piatak and S. Phillips for their assistance in measuring the physical parameters and building the magnet.

References

1. Robert J. Lari, "Magnetic Measurements of Bending Magnets BM-101", Argonne National Laboratory, Particle Accelerator Division Internal Report, RJL-2, September 18, 1962.

2. Robert J. Lari, "Magnetic Measurements of Bending Magnets BM-102", Argonne National Laboratory, Particle Accelerator Division Internal Report, RJL-3, October 1962.

3. Alan M. Winslow, "Magnetic Field Calculations in an Irregular Triangular Mesh", International Symposium on Magnet Technology, SLAC, Sept. 8-10, 1965, pages 170-182.

4. John S. Colonias, Joseph H. Dorst, "Magnet Design Applications of the Magnetostatic Program Called TRIM", International Symposium on Magnet Technology, SLAC, September 8-10, 1965, pages 188-196.

5. H. F. Vogel (Los Alamos Scientific Laboratory, Los Alamos, New Mexico) and R. J. Lari (Argonne National Laboratory, Argonne, Illinois) "Computation of Magnetic End Fields and Comparison with Measurements", see these proceedings.

6. E. C. Berrill, R. S. Odwanzy, "The Use of a High Speed Data Acquisition System in Measuring Large Volume Magnets at the Zero Gradient Synchrotron", 1967 International Conference on Magnet Technology, Oxford, England, pages 675-682.

7. E. C. Berrill, T. W. Hardek, C. E. Buckels, "An Improved High-Speed Data Acquisition System for Steady State or Pulsed Magnetic Field Measurement", 1970 International Conference on Magnet Technology, Hamburg, Germany, May 19-22, 1970; Argonne National Laboratory, Accelerator Division Internal Report ECB/TWH/CEB-1.

8. E. C. Berrill, R. D. George, A. E. Algustyniak, "Organization and Use of a Small-Scale Computer in On- and Off-Line Magnetic Data Processing", 1970 International Conference on Magnetic Technology, Hamburg, Germany, May 19-22, 1970; Argonne National Laboratory, Accelerator Division Internal Report ECB/RDG/AEA-1.

Table I - Magnet Design Data

	Unit	Main Coil	Correction Coil
Gap Height	cm	5	-
Gap Width	cm	50	-
Gap Length	cm	120	-
Coil Turns	-	80	18
Cooling Circuits	-	80	2
Conductor Size	mm		
Septum		4.1 x 4.4	5.8 sq
Return Leg		9.3 sq	-
Cooling Hole Size	mm		
Septum		2.3 dia	3.2 dia
Return Leg		5.2 dia	-

Table II - Magnet Operating Parameters

	Unit	Main Coil	Correction Coil
Central Field	G	17000	-
Current	A	900	200
Terminal Voltage	V	232	12
Power	kW	209	2.4
Water Flow	liters/min.	67.4	2.4
Coil Temperature Rise	^{o}C	40	15
Water Pressure Drop	kg/cm^2	5	5
Current Density	A/mm^2		8.1
Septum		66.4	
Return Leg		14.3	

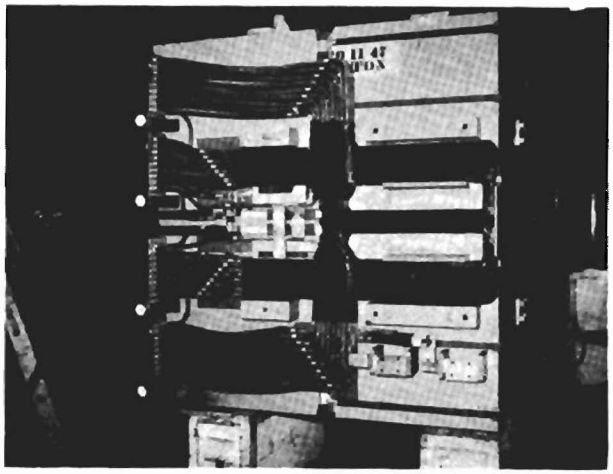

FIGURE 1
Power End of Septum Magnet.
End Guards Removed.

FIGURE 2
Septum Magnet - End Guards Removed.

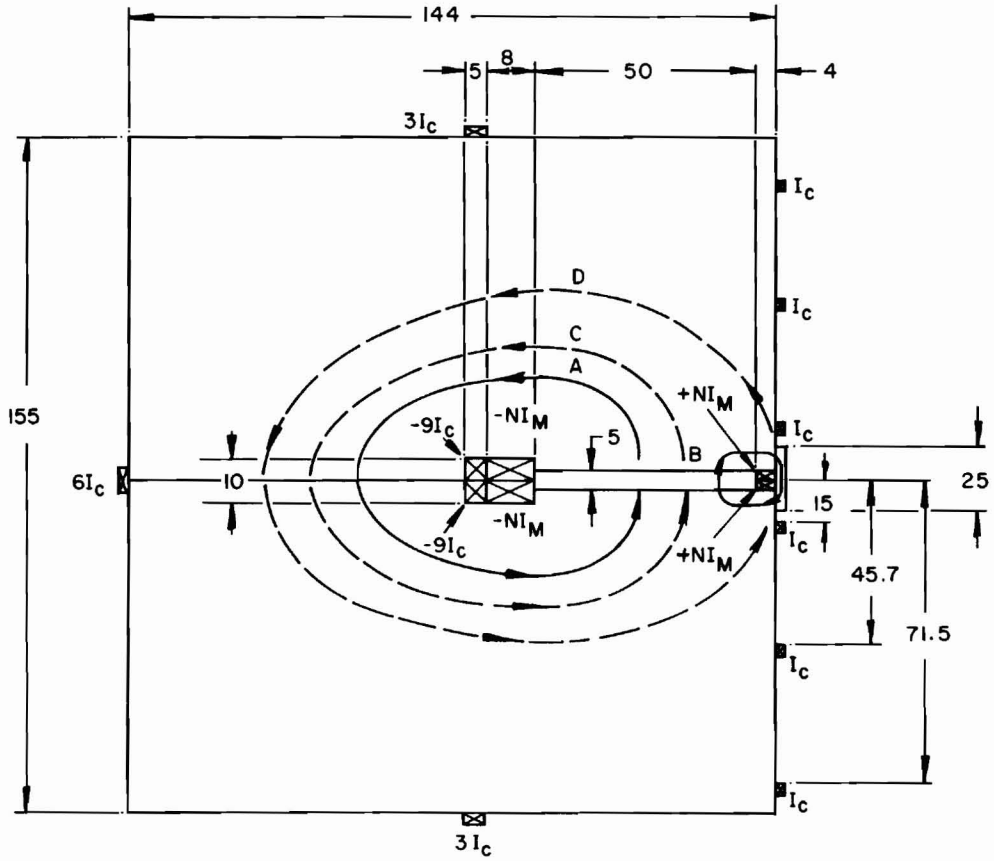

FIGURE 3
SEPTUM MAGNET CROSS-SECTION
DIMENSIONS IN cm.

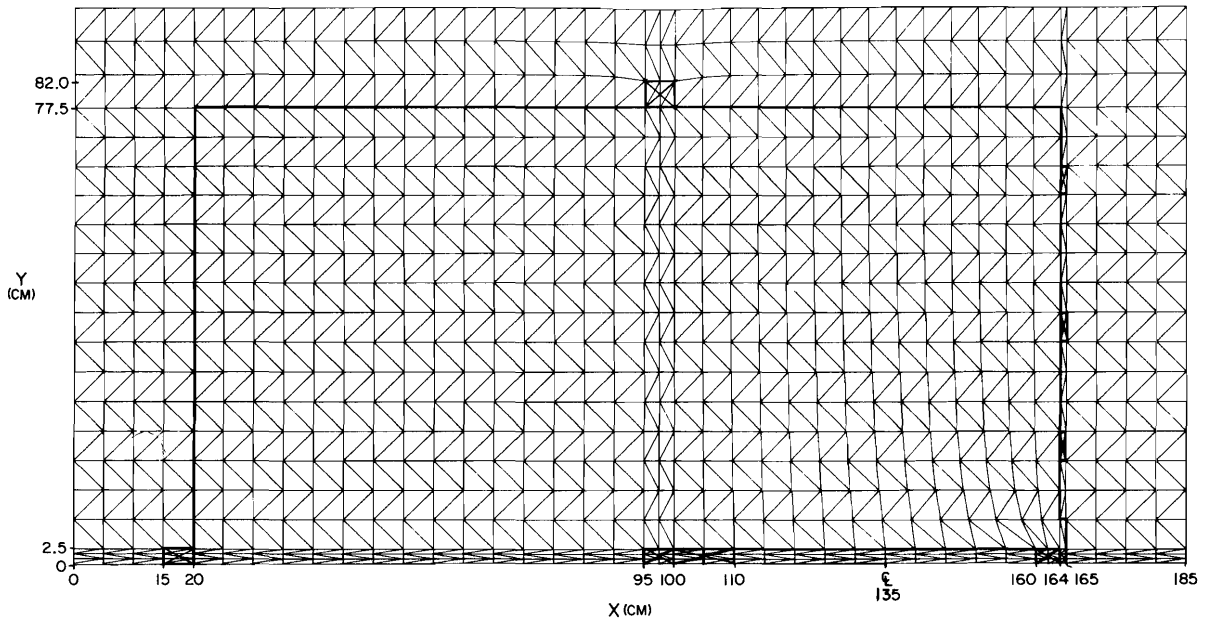

Fig. 4. Triangular Mesh

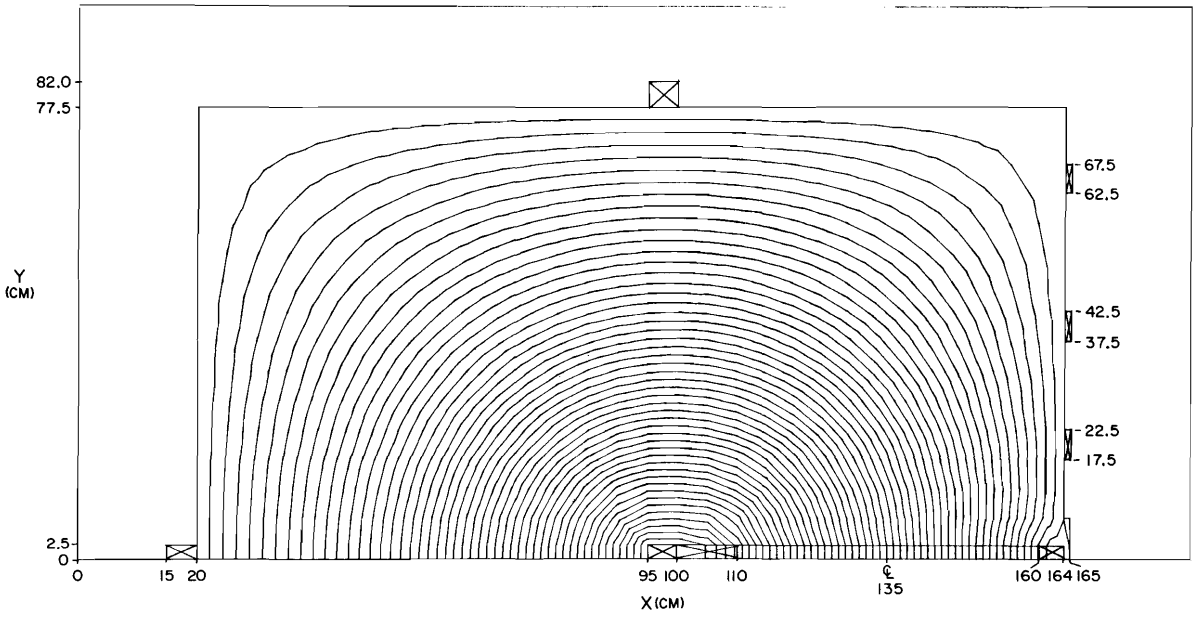

Fig. 5. Flux Lines

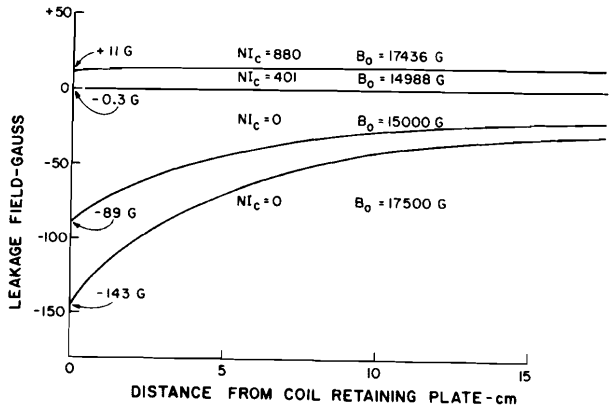

FIGURE 6
LEAKAGE FIELD NEAR THE COIL RETAINING PLATE

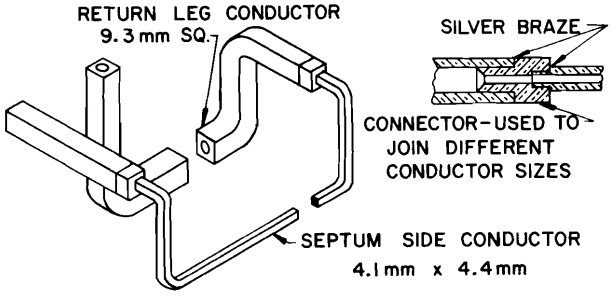

FIGURE 7
TYPICAL MAIN COIL TURN CONSTRUCTION
(NOT TO SCALE)

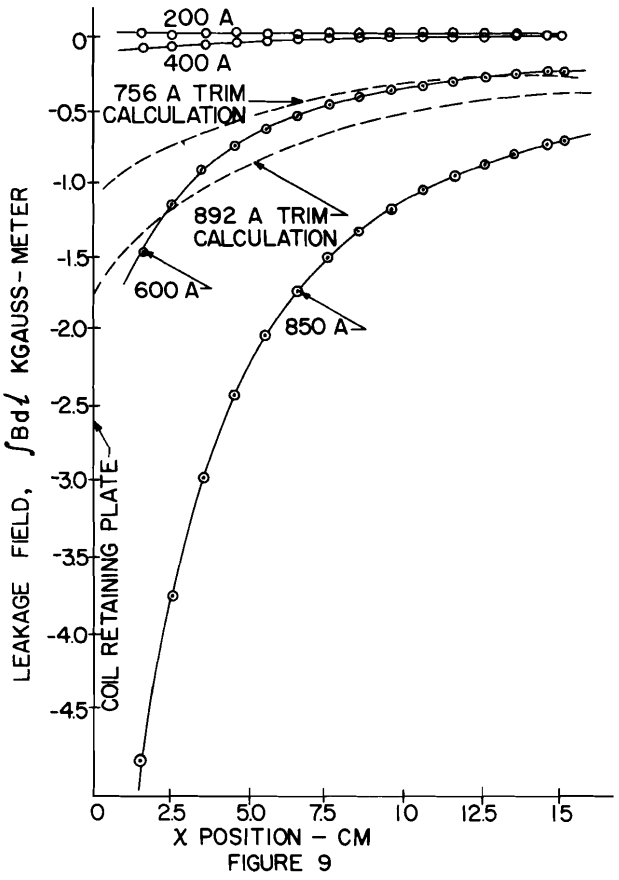

FIGURE 9
LEAKAGE FIELD $\int Bd\ell$ VS. X
(WITHOUT CORRECTION COIL)

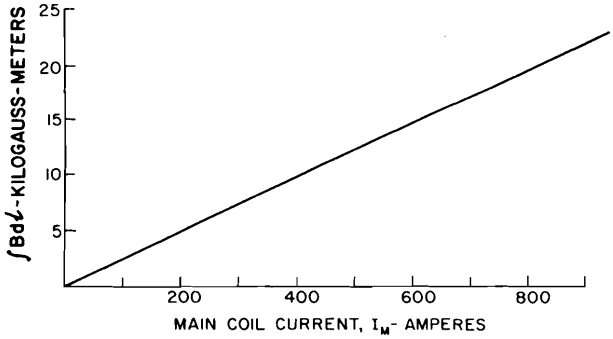

FIGURE 8
CENTRAL $\int Bd\ell$ vs. I_M
(CORRECTION COIL ON)

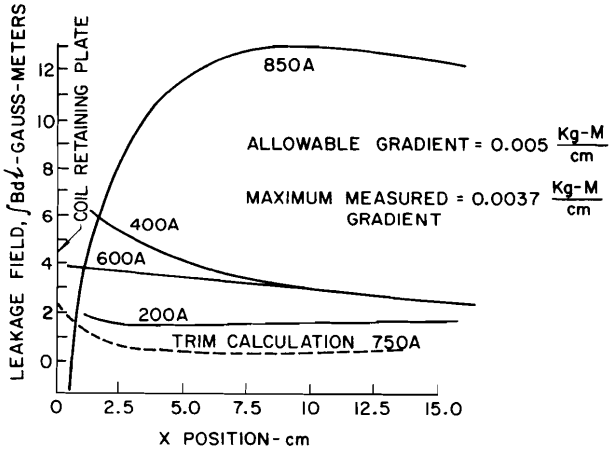

FIGURE 10
LEAKAGE FIELD, $\int Bd\ell$ vs. X
(WITH CORRECTION COIL)

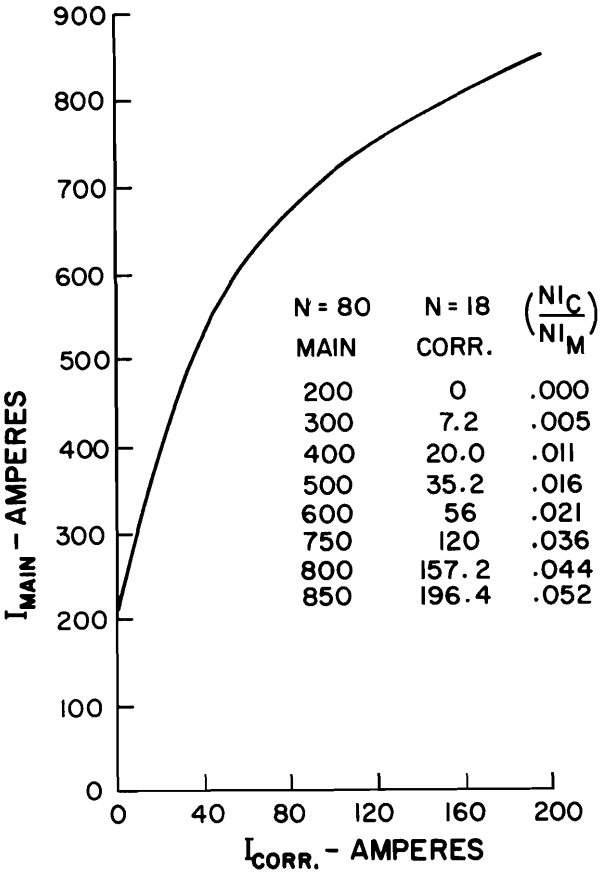

FIGURE 11
OPTIMUM CORRECTION COIL CURRENT

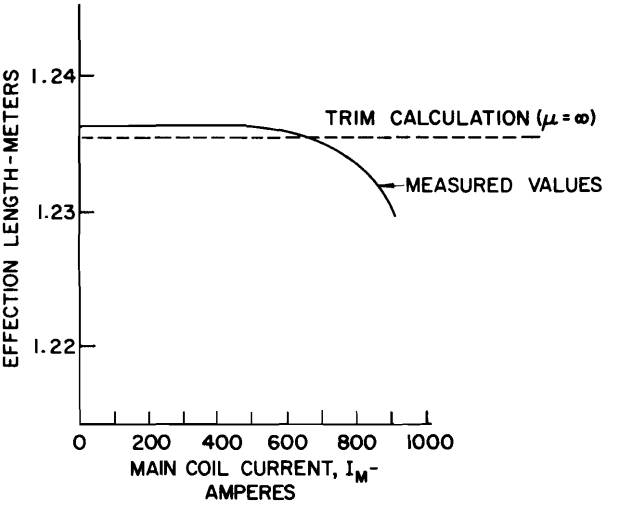

FIGURE 12
EFFECTIVE LENGTH vs. MAIN COIL CURRENT
(CORRECTION COIL ON)